

Synthesis, Characterization, Antioxidative Activity and DNA Binding Properties of the Copper(II), Zinc(II), Nickel(II) Complexes with 1,2-Di(4'-iminonaringenin)ethane

Yong LI, Zheng-yin YANG,* and Tian-rong LI

College of Chemistry and Chemical Engineering and State Key Laboratory of Applied Organic Chemistry, Lanzhou University; Lanzhou 730000, P. R. China.

Received March 23, 2008; accepted August 28, 2008; published online September 1, 2008

A novel naringenin Schiff base ligand (1,2-di(4'-iminonaringenin)ethane, H₆L) and its three transition metal complexes [Cu(II) complex (1), Zn(II) complex (2), and Ni(II) complex (3)] have been prepared and characterized on the basis of elemental analysis, molar conductivity, ¹H-NMR, mass spectra, UV-vis spectra, and IR spectra. The DNA-binding properties of the ligand and its complexes have been investigated by absorption spectroscopy, fluorescence spectroscopy, ethidium bromide (EB) displacement experiments, and viscosity measurement. The results indicated that the ligand and its complexes can bind to DNA. The binding affinity of the Cu(II) complex (1) is higher than that of the ligand and the other two complexes. The intrinsic binding constant (*K_b*) of the complex (1) is 3.3 × 10⁶. In addition, the suppression ratio for O₂⁻ and HO[•] was determined. The 50% inhibition obtained for the ligand and its three complexes demonstrates that, compared to the ligand, the complexes exhibit higher antioxidative activity in the suppression of O₂⁻ and HO[•].

Key words naringenin Schiff base; transition metal complex; antioxidative activity; DNA binding

DNA is an important cellular receptor, many chemicals exert their antitumor effects through binding to DNA thereby changing the replication of DNA and inhibiting the growth of tumor cells.^{1,2)} Then discussing the mechanism of compounds binding to DNA possesses significant meanings. As well-known to all of us, the interaction of small molecular ligands and its transition metal complexes with DNA has been the main subject of intense investigations for almost half of a century.³⁾ Because of the unusual binding properties and general photoactivity, these complexes are suitable candidates as DNA secondary structure probes, antitumor drugs and photocleavers. The design of small complexes that can bind to DNA becomes more and more important.^{4–6)}

It has been proposed that reactive oxygen species (ROS) are involved in the pathogenesis of various diseases, such as lifestyle-related diseases including hypertension⁷⁾ and photoaging due to exposure to ultraviolet radiation.⁸⁾ Free radicals are species that contain unpaired electrons. In the human body, superoxide and hydroxyl radicals are produced by the reduction of oxygen.⁹⁾ Over production of free radicals is considered to be the main contributor to oxidative stress. The oxygen radicals may induce some oxidative damages to biomolecules such as carbohydrates, proteins, lipids, and DNA, thus accelerating aging, cancer, cardiovascular diseases, inflammation and so on.¹⁰⁾

Flavonoids are a large group of phenolic plant constituents. They are broadly distributed in vascular plants and responsible for most of the colors in nature.¹¹⁾ To date, more than 6000 flavonoids have already been identified, although only a smaller number is important from a dietary point of view.¹²⁾ Recently, flavonoids receive considerable attention in the literature, mainly because of their biological and physiological importance.¹³⁾ They are potentially antioxidant, antibacterial, anticancer, anti-inflammatory and antiallergenic agents since they stimulate or inhibit a wide variety of enzyme systems as pharmacological agents.^{14–17)} Naringenin (4',5,7-trihydroxyflavanone) is one of the lesser-known

flavonoids except for its use as antibacterial and anticancer agents.¹⁸⁾ It is a flavanone compound that alters critical cellular processes such as cell multiplication, glucose uptake, and mitochondrial activity.¹⁹⁾

Many transition metals, such as copper, zinc and nickel, are important trace metals in human body. In order to gain more knowledge on naringenin, a new ligand, (1,2-di(4'-iminonaringenin)ethane, H₆L) and its three transition metal complexes were synthesized. The interactions of the ligand and complexes with calf thymus DNA (CT DNA) using absorption spectroscopy, fluorescence spectroscopy, ethidium bromide(EB) displacement experiments, and viscosity measurement were studied for the first time. The antioxidative activity of the ligand and its transition metal complexes was also investigated. Information obtained from present work will be useful to understand the mechanism of interactions of the ligand and complexes with CT DNA and helpful in the development of drugs for curing some diseases.

Experimental

Materials Nitroblue tetrazolium (NBT), methionine (MET), vitamin B₂ (VitB₂), CT DNA and EB were purchased from Sigma Chemical Co. Ethylenediaminetetraacetic acid (EDTA), triethylamine, acetic acid, naringenin, M(NO₃)₂ · nH₂O [M=Cu(II), n=3; Zn(II), n=6; Ni(II), n=6] were produced in China. All chemicals used were of analytical grade. EDTA-Fe(II) and KH₂PO₄-K₂HPO₄ buffers were prepared with doubly deionized water.

All the experiments involved with the interaction of the complexes with CT DNA were carried out in doubly distilled water buffer. The water buffer was produced by mixing 5 mM Tris [Tris(hydroxymethyl)-aminomethane] and 50 mM NaCl with deionized water and adjusted to pH 7.1 with hydrochloric acid. The solution of CT DNA in the buffer gave a ratio of UV absorbance of about 1.8–1.9: 1 at 260 and 280 nm, which indicated that the CT DNA was sufficiently free of protein.²⁰⁾ The CT DNA concentration per nucleotide was determined spectrophotometrically by employing an extinction coefficient of 6600 M⁻¹cm⁻¹ at 260 nm.²¹⁾ The complexes were dissolved in a solvent mixture of 1% *N,N*-dimethylformamide (DMF) and 99% tris-HCl buffer (5 mM tris-HCl, 50 mM NaCl, pH 7.1) at the concentration 1.0 × 10⁻³ M.

Physical Measurements Elemental analyses (C, H, N) were carried out on an Elemental Vario EL analyzer. The metal contents of the complexes were determined by titration with EDTA. The melting point of the com-

* To whom correspondence should be addressed. e-mail: yangzy@lzu.edu.cn

pounds were determined on a Beijing XT4-100X microscopic melting point apparatus. The IR spectra were obtained in KBr discs on a Thermo Mattson FTIR spectrophotometer in the 4000–400 cm^{-1} region. $^1\text{H-NMR}$ spectra were recorded on a Varian VR 200-MHz spectrometer in $\text{DMSO-}d_6$ with TMS (tetramethylsilane) as internal standard. Mass spectra were performed on a APEX II FT-ICR MS instrument using methanol as mobile phase. Conductivity measurements were performed in DMF with a DDS-11C conductometer at 25.0 $^\circ\text{C}$. The UV-vis spectra of the compounds (DMF solution) were recorded on a Varian Cary 100 Cone spectrophotometer. Fluorescence measurements were recorded on a Hitachi RF-4500 spectrofluorophotometer. The absorbance was performed in DMF with a 721-E spectrophotometer in measuring the antioxidative activity of the compounds. Absorption titration experiments were performed with fixed concentration drugs (10 μM), while gradually increasing the concentration of CT DNA. When measuring the absorption spectra, an equal amount of CT DNA was added to both the complex solutions and the reference solution to eliminate the absorbance of CT DNA itself. Each sample solution was scanned in the range 230–400 nm. For all the fluorescence measurements, the entrance and exit slits were both maintained at 10.0 nm. Fixed amounts (10 μM) of the complex **1** were titrated with increasing amounts of CT DNA, over a range of CT DNA concentrations from 0.01 to 0.10 μM . An excitation wavelength of 363 nm was used and the emission intensity was monitored at 437 nm. All the experiments were conducted at 20.0 $^\circ\text{C}$ in a buffer containing 5 mM tris-HCl (pH 7.1) and 50 mM NaCl. Each sample solution was scanned in the range 350–500 nm. Viscosity experiments were conducted on an Ubbelohde viscometer, immersed in a thermostated water-bath maintained to 25.0 $^\circ\text{C}$. Titrations were performed for the Cu(II), Zn(II) and Ni(II) complexes (0.5–3 μM), and each compound was introduced into a CT DNA solution (5 μM) present in the viscometer. Data were presented as $(\eta/\eta_0)^{1/3}$ versus the ratio of the concentration of the compound and CT DNA, where η is the viscosity of CT DNA in the presence of the compound and η_0 is the viscosity of CT DNA alone. Viscosity values were calculated from the observed flow time of CT DNA containing solution corrected from the flow time of buffer alone (t_0), $\eta = t - t_0$.^{22,23)}

Preparation of the Ligand (H_6L) As seen from Fig. 1, a quantity of naringenin (5.9 g, 22 mmol) was dissolved in ethanol (50 cm^3), and then ethylenediamine (0.6 g, 10 mmol) was added dropwise. After 10 min, acetic acid was also added in this solution and the whole was refluxed on an oil bath for one day with stirring. Then the solution became yellow. After cooling and concentrating, a yellow solid separated out. The yellow precipitate was filtered, washed with alcohol, and recrystallized from DMF and H_2O to give the ligand (yield 85%); mp 312–313 $^\circ\text{C}$. The chemical structure of the ligand is shown in Fig. 1. $^1\text{H-NMR}$ ($\text{DMSO-}d_6$, δ , ppm): 2.96 (2H, dd, $J=12.3, 17.0$ Hz, 3'(a)-H), 3.14 (2H, dd, $J=3.0, 17.0$ Hz, 3'(e)-H), 3.70 (4H, m, 1, 2-H), 5.11 (2H, dd, $J=3.0, 12.3$ Hz, 2'-H), 5.60 (2H, s, 6'-H), 5.67 (2H, s, 8'-H), 6.70 (4H, d, $J=8.0$ Hz, 3'', 5''-H), 7.22 (4H, d, $J=8.0$ Hz, 2'', 6''-H), 9.62 (2H, s, 4''-OH, D_2O exchangeable), 9.76 (2H, s, 7''-OH, D_2O exchangeable), 15.60 (2H, s, 5'-OH, D_2O exchangeable). *Anal.* Calcd for $\text{C}_{32}\text{H}_{28}\text{N}_2\text{O}_8$: C, 67.60; H 4.96; N 4.93. Found: C, 67.73; H 4.82; N 4.86. IR (KBr): 3354, 1594 cm^{-1} .

Preparation of the Complexes The ligand (56.8 mg, 0.1 mmol) was dissolved in ethanol (20 ml) and $\text{Cu}(\text{NO}_3)_2 \cdot 3\text{H}_2\text{O}$ (24.5 mg, 0.1 mmol) was then added. After 5 min, triethylamine (20.2 mg, 0.2 mmol) was added and the solution was stirred for one day at room temperature. Then a brown precipitate, Cu complex (**1**) was separated by suction filtration. It was purified by washing six times with ethanol, and dried for 48 h in vacuum. The Zn(II) complex (**2**) and Ni(II) complex (**3**) were also synthesized as the above method.

Complex (1): Yield, 65%. *Anal.* Calcd for $\text{C}_{32}\text{H}_{26}\text{CuN}_2\text{O}_8$: C, 61.00; H, 4.16; N, 4.45; Cu, 10.09. Found: C, 60.98; H, 4.22; N, 4.40; Cu, 10.13. IR (KBr): 3279, 1587, 598, 490 cm^{-1} . A_m (DMF): 1.2 $\text{S cm}^2 \text{mol}^{-1}$. **Complex (2):** Yield, 72%. *Anal.* Calcd for $\text{C}_{32}\text{H}_{26}\text{N}_2\text{O}_8\text{Zn}$: C, 60.82; H, 4.15; N, 4.43; Zn, 10.35. Found: C, 61.02; H, 4.26; N, 4.50; Zn, 10.45. IR (KBr): 3270, 1585, 586, 486 cm^{-1} . A_m (DMF): 4.3 $\text{S cm}^2 \text{mol}^{-1}$. **Complex (3):** Yield, 63%. *Anal.* Calcd for $\text{C}_{32}\text{H}_{26}\text{N}_2\text{NiO}_8$: C, 61.47; H, 4.19; N, 4.48; Ni, 9.39. Found: C, 61.42; H, 4.28; N, 4.43; Ni, 9.32. IR (KBr): 3269, 1585, 599, 503 cm^{-1} . A_m (DMF): 2.4 $\text{S cm}^2 \text{mol}^{-1}$.

Results and Discussion

Characterization of Complexes The complexes are air stable for at least six months and easily soluble in DMF and DMSO; slightly soluble in acetone, chloroform, methanol

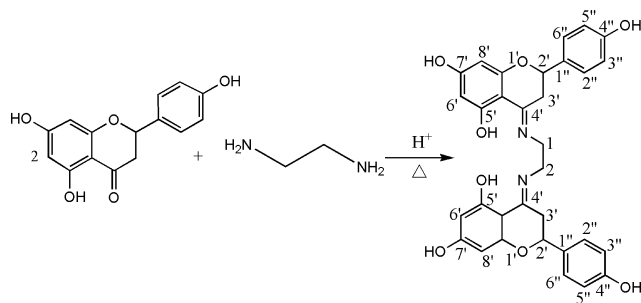


Fig. 1. Preparation Route of the Ligand (H_6L)

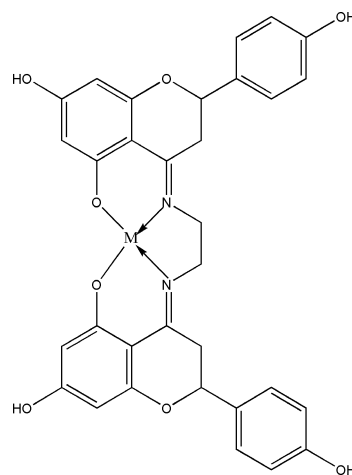


Fig. 2. Proposed Structure of the Complexes

M=Cu, Zn, and Ni.

and ethanol; insoluble in benzene, water and diethyl ether. The molar conductance values of the complexes are in the range of 1.2–4.3 $\text{S cm}^2 \text{mol}^{-1}$ in DMF, which show that all the complexes are non-electrolytes in DMF.²⁴⁾ The element analyses show that the formulas for the complexes are H_4ML (M=Cu, Zn, and Ni).

IR spectra provide a quantity of valuable information on coordination reaction. All the spectra are characterized by vibrational bands mainly due to the OH and C=N. The $\nu(\text{O-H})$ for the ligand appears at 3354 cm^{-1} , and this peak for the complexes shifts at 3270 cm^{-1} or so. The $\nu(\text{C=N})$ vibration of the free ligand is at 1594 cm^{-1} . For the complexes, the bands occur at 1585 cm^{-1} or so, which makes a shift towards lower frequency by 9 cm^{-1} . It shows that the nitrogen atom takes part in the coordination.²⁵⁾ Weak bands at 490 cm^{-1} or so are assigned to $\nu(\text{M-N})$. It confirms that the nitrogen atom of the imino-group bands to metal ion. Concerning the complexes, the band at 598 cm^{-1} or so is assigned to $\nu(\text{M-O})$, demonstrating that the oxygen of hydroxyl group has formed a coordinative bond with metal ion.^{26–28)} On the basis of all these data, the likely structure of the complexes is shown in Fig. 2.

Electrospray ionization (ESI) mass spectrum of the Cu(II) complex (**1**) is shown in Fig. 3 and the proposed degradation of the Cu(II) complex (**1**) that could be explained on the basis of the fragmentation pattern is displayed in Fig. 4. The mass spectrum of complex **1** shows peaks at m/z of 630.1, 537.7, 453.2, 437.2, and 400.9, respectively. ESI-MS: $m/z = 630 [\text{M}+\text{H}]^+$.

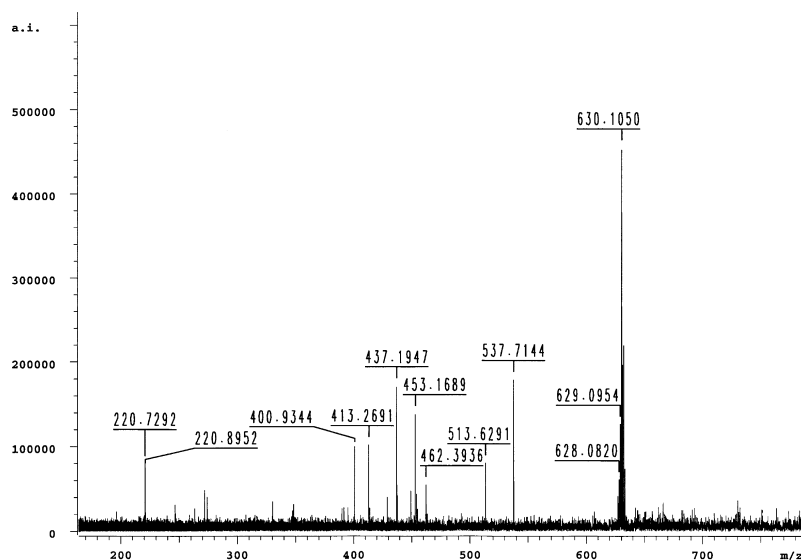


Fig. 3. Electrospray Ionization (ESI) Mass Spectrum of the Cu(II) Complex (1)

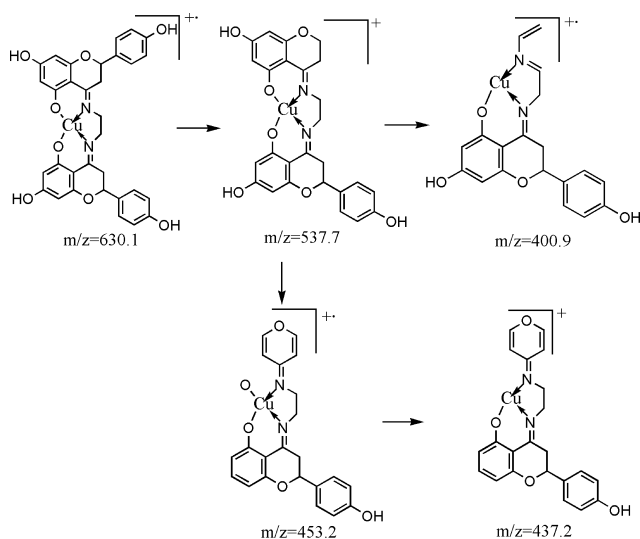


Fig. 4. Proposed Degradation of the Cu(II) Complex (1)

Electronic Absorption Spectroscopy Electronic absorption spectroscopy is widely applied to determine the binding characteristics of metal complex with DNA. Intercalative mode of binding usually results in hypochromism and red shift because of the strong stacking interaction between an aromatic chromophore and the base pairs of DNA. The extent of the spectral change is related to the strength of binding.²⁹⁾

For complex **1**, with the increase of DNA concentration, hypochromism reaches 12.5% at 243 nm and 19.3% at 314 nm. Complex **2** also appears with different hypochromism of 23.2% at 240 nm and 41.2% at 316 nm. The complex **3** exhibits hypochromism of 15.6% at 345 nm and 25.1% at 265 nm, respectively. Likewise, with the increase of DNA concentrations, the absorption bands at 237 nm and 320 nm for the ligand appear with hypochromism of 10.8% and 7.9%, respectively. Accompanied with hypochromisms, the bands of the four compounds are all gotten a small red shift by less than 3 nm. The above phenomena suggest that these compounds can interact with CT DNA by intercalating the

compounds into the base pairs of the double helical DNA.^{30–32)}

To compare quantitatively the affinity of these four compounds binding to DNA, K_b has been estimated. From absorption data, K_b was determined by using the following equation through a plot of $[DNA]/(\epsilon_a - \epsilon_f)$ versus $[DNA]$

$$[DNA]/(\epsilon_a - \epsilon_f) = [DNA]/(\epsilon_b - \epsilon_f) + 1/[K_b(\epsilon_b - \epsilon_f)]$$

where $[DNA]$ is the concentration of DNA, ϵ_a , ϵ_f and ϵ_b are, respectively, the apparent extinction coefficient ($A_{\text{obsd}}/[\text{compound}]$), the extinction coefficient for free compound and the extinction coefficient for compound in the fully bound form. In plots of $[DNA]/(\epsilon_a - \epsilon_f)$ versus $[DNA]$, K_b is given by the ratio of the slope to the intercept.³³⁾

From Fig. 5, K_b obtained for complex **2** is $1.4 \times 10^6 \text{ M}^{-1}$. Likewise, K_b of complex **1**, complex **3** and the ligand is 3.3×10^6 , 1.0×10^6 and $6.0 \times 10^5 \text{ M}^{-1}$, respectively. Comparing K_b of these compounds with that of other DNA-intercalative complexes, K_b of $[\text{Cr}(\text{DPPZ})_2\text{Cl}_2]\text{ClO}_4$ is $(1.8 \pm 0.5) \times 10^7 \text{ M}^{-1}$ ³⁴⁾; K_b of $[\text{Ru}(\text{bpy})_2(\text{DMHBT})]\text{Cl}_2$ and $[\text{Ru}(\text{phen})_2(\text{DMHBT})]\text{Cl}_2$ are $(2.87 \pm 0.2) \times 10^4$ and $(1.01 \pm 0.2) \times 10^5 \text{ M}^{-1}$, respectively³⁵⁾; K_b of $[\text{EuL}_2(\text{NO}_3)_2]\text{NO}_3$ ³⁶⁾ and $[(\text{phen})\text{Cu}(\mu\text{-bipp})\text{Cu}(\text{phen})]^{4+}$ ³⁷⁾ are $3.55 \times 10^6 \text{ M}^{-1}$ and $1.6 \times 10^4 \text{ M}^{-1}$ respectively; K_b of $[\text{Ru}(\text{bpy})_2(\text{ptdb})](\text{ClO}_4)_2$, $[\text{Ru}(\text{bpy})_2(\text{ptda})](\text{ClO}_4)_2$, and $[\text{Ru}(\text{bpy})_2(\text{ptdp})](\text{ClO}_4)_2$ are $(1.9 \pm 0.2) \times 10^4$, $(3.1 \pm 0.3) \times 10^4$, and $(5.9 \pm 0.2) \times 10^4$, respectively.³⁸⁾ From the data, we deduce that these compounds can bind to DNA by intercalation. The values of K_b also indicate that the binding strength of complex **1** is stronger than those ones of ligand and the other two complexes.

Fluorescence Spectra The free ligand and complex **1**, **2** and **3** can emit weak luminescence in Tris buffer with a maximum wavelength of about 450 nm. The enhancements in the emission intensity of complex **2** with increasing CT DNA concentrations are shown in Fig. 6. As seen from Fig. 6, the intensity of emission at 440 nm increases notably in the presence of CT DNA. For complex **1**, **2**, **3** and free ligand, the emission intensities of the four compounds grow to around 1.25, 1.23, 1.21, and 1.17 times larger, respectively, than those in the absence of DNA.

The enhancements of emission intensity imply that these

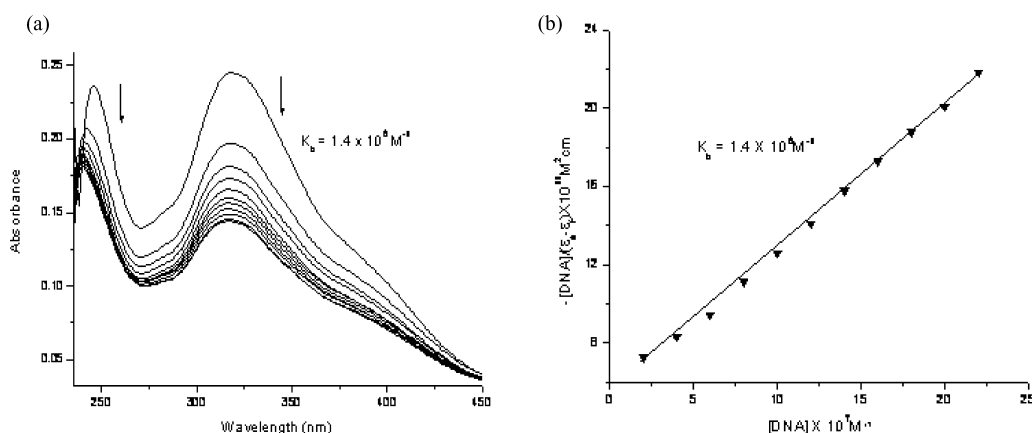


Fig. 5. (a) Absorption Spectra of Zn(II) Complex (2) ($10 \mu\text{M}$) in the Absence (Top Spectrum) and Presence of Increasing Amounts of Calf Thymus DNA (0.25, 0.50, 0.75, 1.00, 1.25, $1.50 \mu\text{M}$; Subsequent Spectra)

Arrow shows the absorbance changes upon increasing DNA concentration.

(b) Plot of $[\text{DNA}]/(\epsilon_a - \epsilon_f)$ versus $[\text{DNA}]$ for the Titration of Complex 2 with CT DNA

▼, experimental data points; full lines, linear fitting of the data. Intrinsic binding constant $K_b = 1.4 \times 10^6 \text{M}^{-1}$.

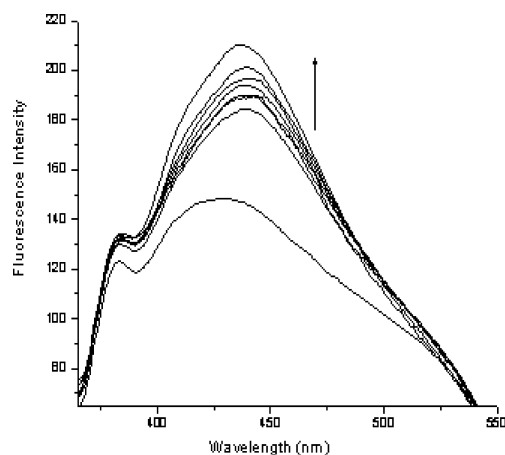


Fig. 6. Emission Enhancement Spectra of Zn(II) Complex (2) ($10 \mu\text{M}$) in the Absence (Bottom Spectrum) and Presence of Increasing Amounts of Calf Thymus DNA (0.01, 0.02, 0.03, 0.04, 0.05, $0.06 \mu\text{M}$; Subsequent Spectra) Respectively

Arrow shows the emission intensity changes upon increasing DNA concentration.

compounds can insert between DNA base pair. As a result, these compounds are protected from solvent water molecules by the hydrophobic environment inside the DNA helix; the accessibility of solvent water molecules to these compounds is reduced. The binding of these four compounds to DNA leading to a marked increase in emission intensity also agrees with those observed for other intercalators.³⁹⁾ Compared to the intensity enhancement of these compounds in the presence of DNA, complex 1 can bind to DNA more strongly than complex 2, 3 and the ligand.

Further support for the ligand and complexes binding to DNA *via* intercalation is given through the emission quenching experiment. EB is a common fluorescent probe for DNA structure and has been employed in examinations of the mode and process of metal complex binding to DNA.⁴⁰⁾ A 2.5 ml solution of $4 \mu\text{M}$ DNA and $0.32 \mu\text{M}$ EB was titrated by 5–50 μM the complexes and ligand. Quenching data were analyzed according to the Stern–Volmer equation, which could be used to determine the fluorescent quenching mecha-

nism:

$$F_0/F = 1 + K_q[Q]$$

where F_0 and F are the fluorescence intensity in the absence and in the presence of drug at $[Q]$ concentration respectively; K_q is the quenching constant and $[Q]$ is the quencher concentration. Plots of F_0/F versus $[Q]$ appear to be linear and K_q depends on temperature.⁴¹⁾

It is well known that EB can intercalate nonspecifically into DNA which causes it to fluoresce strongly and the fluorescence-based competition technique can provide indirect evidence for the DNA binding mode. The emission band of the DNA–EB system decreased in intensity with an increase of the compounds concentrations, which indicated that the compounds can displace EB from DNA–EB system. From Fig. 7, the K_q value of the Zn(II) complex is $4.16 \times 10^4 \text{M}^{-1}$. Likewise, the K_q values of the Cu(II) complex, Ni(II) complex and ligand are 7.14×10^4 , 3.13×10^4 and $2.02 \times 10^4 \text{M}^{-1}$ respectively. The data show that the interaction of the complexes is stronger than that of the ligand, which is consistent with the above absorption spectral results. It can be concluded that the complexes and free ligand insert into DNA by intercalation.

Viscosity Measurement In order to further clarify the interactions between the compounds and DNA, viscosity measurements were carried into execution. Hydrodynamic measurements that are sensitive to length change (*i.e.* viscosity and sedimentation) are regarded as the least ambiguous and the most critical tests of binding in solution in the absence of crystallographic structural data.⁴²⁾ Figure 8 shows the relative viscosity of DNA ($30 \mu\text{M}$) in the presence of varied amounts of the ligand and its three transition metal complexes. Viscosity experimental results clearly show that all the compounds can intercalate between adjacent DNA base pairs, causing an extension in the helix, and thus increase the viscosity of DNA⁴³⁾; and the Cu(II) complex can intercalate more strongly and deeply than the free ligand, leading to the greater increase in viscosity of the DNA with an increasing concentration of complex. The results obtained from viscosity studies are consistent with those obtained from spectro-

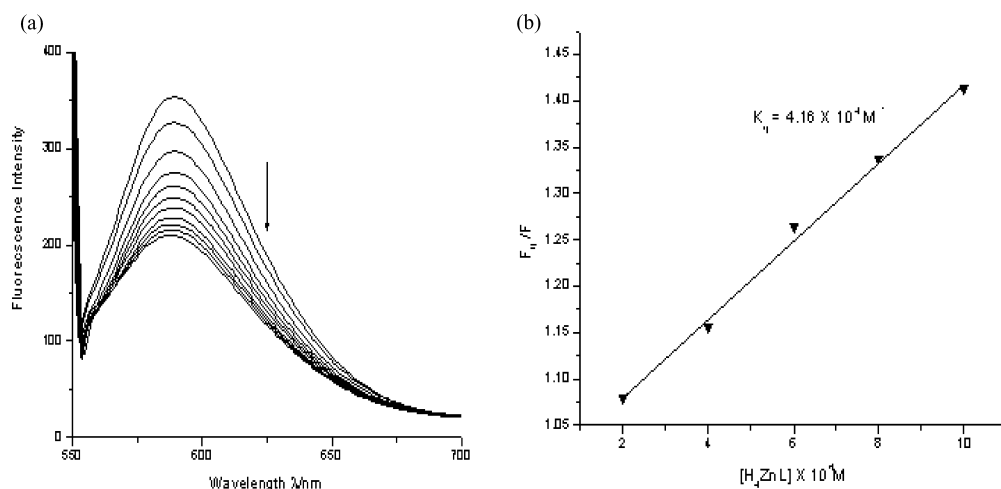


Fig. 7. (a) The Emission Spectra of DNA-EB System, in the Presence of 0, 2, 4, 6, 8, 10, 12, 14, 16, 18, 20 μM Zn(II) Complex (2)

Arrow shows the emission intensity changes upon increasing concentration.

(b) Plot of F_0/F versus $[H_2ZnL]$

▼, experimental data points; full lines, linear fitting of the data. Inset: Stern Volmer plot of the fluorescence titration data of Zn(II) complex (2). $K_q = 4.16 \times 10^4 M^{-1}$.

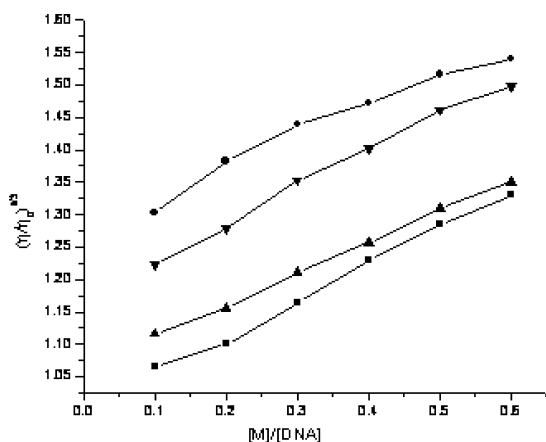


Fig. 8. Effect of Increasing Amounts of the Ligand and Complexes on the Relative Viscosity of CT DNA at 25.0 °C

■, experimental data points of the ligand; ●, experimental data points of Cu(II) complex; ▼, experimental data points of Zn(II) complex; ▲, experimental data points of Ni(II) complex.

scopic studies.

Scavenger Measurements of $O_2^{\cdot -}$ The superoxide radical ($O_2^{\cdot -}$) was produced by the system MET/VitB₂/NBT.⁴⁴ The amount of $O_2^{\cdot -}$ and suppression ratio for $O_2^{\cdot -}$ can be calculated by measuring the absorbance at 560 nm, because NBT can be reduced quantitatively to blue formazan by $O_2^{\cdot -}$. The solution of MET, VitB₂ and NBT was prepared with 0.067 M phosphate buffer (pH=7.8) at the condition of avoiding light. The tested compounds were dissolved in DMF. The reaction mixture contained MET (0.01 mol l⁻¹), NBT (4.6×10^{-5} mol l⁻¹), VitB₂ (3.3×10^{-6} mol l⁻¹), phosphate buffer solution (0.067 mol l⁻¹), and the tested compound (the final concentration: $C_{i(i=1-5)} = 0.4, 1.0, 2.0, 4.0, 6.0 \mu M$). After incubating at 30 °C for 10 min and illuminating with a fluorescent lamp for 3 min, the absorbance (A_i) of the samples were measured at 560 nm. The sample without the tested compound and avoiding light was used as the control. The suppression ratio for $O_2^{\cdot -}$ was calculated from the following expression:

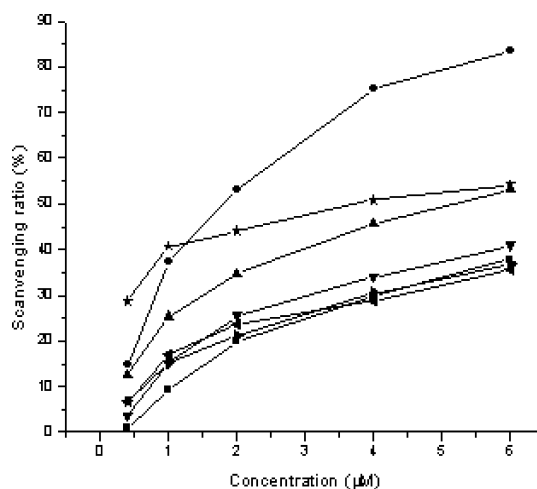


Fig. 9. Scavenging Effect of the Ligand and Complexes on $O_2^{\cdot -}$

■, experimental data points of the ligand; ●, experimental data points of Cu(II) complex; ▼, experimental data points of Zn(II) complex; ▲, experimental data points of Ni(II) complex; ★, experimental data points of Cu(NO₃)₂·3H₂O; ◆, experimental data points of Zn(NO₃)₂·6H₂O; ►, experimental data points of Ni(NO₃)₂·6H₂O.

$$\text{suppression ratio (\%)} = [(A_0 - A_i)/A_0] \times 100$$

where A_i = the absorbance in the presence of the ligand or its complexes, A_0 = the absorbance in the absence of the ligand or its complexes.

Figure 9 and Table 1 depict the inhibitory effect of the compounds on $O_2^{\cdot -}$. The average suppression ratio for $O_2^{\cdot -}$ increases with the increase of the compound concentration in the range of tested concentration. The average suppression ratio of the ligand ($IC_{50} = 14.969 \mu M$) is the least in all the compounds. The Cu(II) complex (1) ($IC_{50} = 1.568 \mu M$) is the most effective inhibitor in these complexes, whereas the Zn(II) complex (2) is the poorest one. The improvement of the naringenin schiff base ligand may be explained by the redox behavior of the metal. The average suppression ratio of the metal salts is weaker than that of the corresponding com-

Table 1. The Influence of Investigated Compounds for O_2^-

Compound	Average inhibition (%) for O_2^-					Equation	IC_{50} , μM	R^2
	0.4 μM	1.0 μM	2.0 μM	4.0 μM	6.0 μM			
H ₆ L	1.1	9.3	20.0	29.7	37.9	$y=32.53x+11.77$	14.969	0.968
H ₄ CuL	14.8	37.4	53.1	75.3	83.5	$y=61.96x+37.90$	1.568	0.994
H ₄ ZnL	3.7	15.2	25.5	34.0	40.9	$y=32.75x+15.97$	9.063	0.991
H ₄ NiL	12.6	25.3	34.7	45.6	53.2	$y=35.55x+25.72$	4.820	0.987
Cu(NO ₃) ₂ ·3H ₂ O	28.8	40.7	44.1	50.9	54.2	$y=20.85x+38.39$	10.876	0.981
Zn(NO ₃) ₂ ·6H ₂ O	6.8	17	23.7	28.8	35.6	$y=23.37x+16.39$	27.416	0.991
Ni(NO ₃) ₂ ·6H ₂ O	6.8	15.2	21.3	30.5	36.9	$y=25.30x+15.84$	22.397	0.991

IC_{50} values were calculated from regression lines where: x was log of the tested compound concentration and y was percent inhibition of the tested compounds. When the percent inhibition of the tested compounds was 50%, the tested compound concentration was IC_{50} . R^2 =correlation coefficient.

Table 2. The Influence of Investigated Compounds for OH \cdot

Compound	Average inhibition (%) for OH \cdot					Equation	IC_{50} , μM	R^2
	1.0 μM	2.0 μM	3.0 μM	4.0 μM	5.0 μM			
H ₆ L	5.4	23.8	33.3	45.2	54.8	$y=73.00x+1.54$	4.611	0.991
H ₄ CuL	49.6	59.5	69.0	78.6	88.1	$y=53.67x+46.64$	1.155	0.951
H ₄ ZnL	35.7	47.6	61.9	69.1	83.3	$y=65.43x+32.31$	1.864	0.951
H ₄ NiL	16.7	31.0	42.9	50.0	61.9	$y=62.24x+14.62$	3.702	0.975
Mannitol	2.3	12.5	24.6	32.9	43.1	$y=57.26x-0.73$	10.190	0.958
Cu(NO ₃) ₂ ·3H ₂ O	27.9	42.4	47.3	53.3	59.4	$y=43.23x+28.08$	3.214	0.990
Zn(NO ₃) ₂ ·6H ₂ O	18.2	33.9	41.2	49.7	54.6	$y=51.79x+17.99$	4.150	0.997
Ni(NO ₃) ₂ ·6H ₂ O	2.4	16.3	25.3	32.4	38.7	$y=51.44x+1.63$	8.716	0.996

IC_{50} values were calculated from regression lines where: x was log of the tested compound concentration and y was percent inhibition of the tested compounds. When the percent inhibition of the tested compounds was 50%, the tested compound concentration was IC_{50} . R^2 =correlation coefficient.

plexes. It is clear that the scavenger effect on O_2^- can be enhanced by the formation of metal–ligand complexes and the metal ions also affect the ability. Due to their lower values of IC_{50} , they are potential drugs to eliminate the radicals.

Hydroxy Radical Scavenging Activity The hydroxyl radical in aqueous media was generated through the Fenton reaction.⁴⁵⁾ The solution of the tested compound was prepared with DMF. The sample contained 2.5 ml of 0.15 M phosphate buffer (pH=7.4), 0.5 ml of 114 μM safranin, 1 ml of 945 μM EDTA–Fe(II), 1 ml of 0.3% H₂O₂, and 25 μl solution of the tested compound (the final concentration: C_i ($i=1-5$)=1.0, 2.0, 3.0, 4.0, 5.0 μM). The sample without the tested compound was used as the control. The reaction mixtures were incubated at 37 °C for 60 min in a water-bath. Absorbances (A_i , A_0 , A_c) at 520 nm were measured. The suppression ratio for HO \cdot was calculated from the following expression:

$$\text{suppression ratio (\%)} = [(A_i - A_0) / (A_c - A_0)] \times 100$$

where A_i =the absorbance in the presence of the tested compound; A_0 =the absorbance in the absence of the tested compound; A_c =the absorbance in the absence of the tested compound, EDTA–Fe(II), H₂O₂.

The data of suppression ratio for OH \cdot are shown in Fig. 10 and Table 2. The inhibitory effect of the compounds is marked and the average suppression ratio for OH \cdot increases with the increase of the compound concentration. The average suppression ratio of the ligand (IC_{50} =4.611 μM) is the poorest in all the compounds and Cu(II) complex (IC_{50} =1.155 μM) is the most effective one. In addition, the average suppression ratio of the metal salts is weaker than that of the corresponding complexes. It indicates that be-

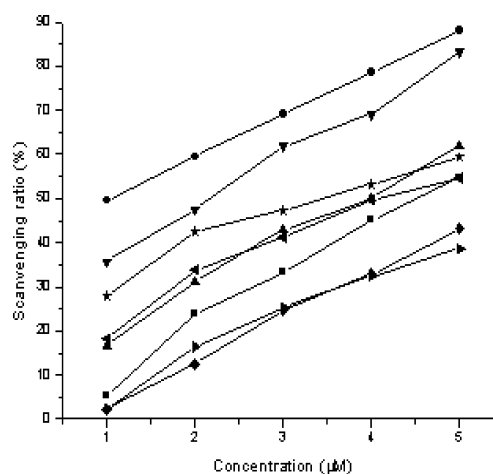


Fig. 10. Scavenging Effect of the Ligand, Complexes and Mannitol on HO \cdot

■, experimental data points of the ligand; ●, experimental data points of Cu(II) complex; ▼, experimental data points of Zn(II) complex; ▲, experimental data points of Ni(II) complex; ◆, experimental data points of mannitol; ★, experimental data points of Cu(NO₃)₂·3H₂O; ◄, experimental data points of Zn(NO₃)₂·6H₂O; ►, experimental data points of Ni(NO₃)₂·6H₂O.

cause of the formation of coordination compounds, the scavenger effect can be enhanced. Moreover, mannitol is a well known natural antioxidant, so the scavenging effect of mannitol against hydroxyl radical is also studied by using the same method. As shown in Table 2, the 50% inhibition concentration value of mannitol is 10.7 μM , which is more than that of the ligand and complexes. They are potential drugs for some diseases.

Conclusion

Taken together, the ligand and its three transition metal complexes have been synthesized and characterized by several methods. The interaction of the ligand and complexes with CT DNA was investigated by absorption, fluorescence and viscosity measurements. K_b shows that complex **1** ($3.3 \times 10^6 \text{ M}^{-1}$), complex **2** ($1.4 \times 10^6 \text{ M}^{-1}$) and complex **3** ($1.0 \times 10^6 \text{ M}^{-1}$) bind to CT DNA more avidly than the free ligand ($6.0 \times 10^5 \text{ M}^{-1}$). In addition, the compounds have active scavenging effect on O_2^- and OH^\cdot . Information obtained from present work will be useful to understand the mechanism of complexes with CT DNA and helpful in the development of potential biological and physiological appliance in the future.

Acknowledgements This work is supported by the National Natural Science Foundation of China (20475023) and Gansu NSF (0710RJZA012).

References

- Friedman A. E., Kumar C. V., Turro N. J., Barton J. K., *Nucleic Acids Res.*, **19**, 2595—2602 (1991).
- Pyle A. M., Morii T., Barton J. K., *J. Am. Chem. Soc.*, **112**, 9432—9434 (1990).
- Dervan P. B., *Biorg. Med. Chem.*, **9**, 2215—2235 (2001).
- Chan S., Wong W. T., *Coord. Chem. Rev.*, **138**, 219—296 (1995).
- Pratviel G., Bernadou J., Meunier B., *Adv. Inorg. Chem.*, **45**, 251—312 (1998).
- Liang F., Wang P., Zhou X., Li T., Li Z. Y., Lin H. K., Gao D. Z., Zheng C. Y., Wu C. T., *Bioorg. Med. Chem. Lett.*, **14**, 1901—1904 (2004).
- Towyz M. R., *Hypertension*, **44**, 248—252 (2004).
- Fujimori T., Yamada S., Yasui H., Sakurai H., In Y., Ishida T., *J. Biol. Inorg. Chem.*, **10**, 831—841 (2005).
- Banerjee A., Dasgupta N., De B., *Food Chem.*, **90**, 727—733 (2005).
- Proctor P. H., Reynolds E. S., *Physiol. Chem. Phys. Med. NMR*, **16**, 175—195 (1984).
- Knekt P., Jarvinen R., Seppanen R., Heliovaara M., Pukkala L. T., Aromaa A., *Am. J. Epidemiol.*, **146**, 223—230 (1997).
- Erlund I., *Nutr. Res.*, **24**, 851—874 (2004).
- Sakaguchi Y., Maehara Y., Baba H., Kusumoto T., Sugimachi K., Newmanv R., *A. Cancer Res.*, **52**, 3306—3309 (1992).
- Habtemariam S., *J. Nat. Prod.*, **60**, 775—778 (1997).
- Aljancic I., Vajs V., Menkovic N., Karadzic I., Juranic N., Milosavljevic S., Macura S., *J. Nat. Prod.*, **62**, 909—911 (1999).
- Ko F., Chu C., Lin C., Chang C., Teng C., *Biochim. Biophys. Acta*, **1389**, 81—90 (1998).
- Nkengfack A., Vouffo T., Fomun Z., Meyer M., Bergendorff S. O., *Phytochemistry*, **36**, 1047—1051 (1994).
- Ramaswamy A. S., Jayaraman S., Sirsi M., Rao K. H., *Indian J. Exp. Biol.*, **10**, 72—73 (1972).
- Misty R., Raquel M., Hind A., Paul A. S., *Biochem. Biophys. Res. Commun.*, **345**, 516—522 (2006).
- Satyanarayana S., Dabrowiak J. C., Chaires J. B., *Biochemistry*, **31**, 9319—9324 (1992).
- Kumar C. V., Asuncion E. H., *J. Am. Chem. Soc.*, **115**, 8547—8553 (1993).
- Eriksson M., Leijon M., Hiort C., Norden B., Gradsland A., *Biochemistry*, **33**, 5031—5040 (1994).
- Xiong Y., He X. F., Zou X. H., Wu J. Z., Chen X. M., Ji L. N., Li R. H., Zhou J. Y., Yu R. B., *J. Chem. Soc. Dalton Trans.*, **1**, 19—24 (1999).
- Geary W. J., *Coord. Chem. Rev.*, **7**, 81—122 (1971).
- Narang K., Singh V. P., *Transition Met. Chem.*, **18**, 287—290 (1993).
- Yang Z. Y., Yang R. D., Li Q., Li F. S., *Synth. React. Inorg. Met.-Org. Chem.*, **29**, 205—214 (1999).
- Yang Z. Y., *Synth. React. Inorg. Met.-Org. Chem.*, **32**, 903—912 (2002).
- Maarchetti F., Pettinari C., Pettinari R., Leonesi D., Lorenzotti A., *Polyhedron*, **18**, 3041—3050 (1999).
- Xu Z. D., Liu H., Xiao S. L., Yang M., Bu X. H., *J. Inorg. Biochem.*, **90**, 79—84 (2002).
- Wu J. Z., Yuan L., Wu J. F., *J. Inorg. Biochem.*, **99**, 2211—2216 (2005).
- Sharma S., Singh S. K., Chandra M., Pandey D. S., *J. Inorg. Biochem.*, **99**, 458—466 (2005).
- Zhao G. H., Li F. H., Lin H., Lin H. K., *Bioorg. Med. Chem.*, **15**, 533—540 (2007).
- Xu H., Zheng K. C., Lin L. J., Li H., Gao Y., Ji L. N., *J. Inorg. Biochem.*, **98**, 87—97 (2004).
- Vaidyanathan G. V., Balachandran U. N., *J. Inorg. Biochem.*, **95**, 334—342 (2003).
- Lawrence D., Vaidyanathan V. G., Nair B. U., *J. Inorg. Biochem.*, **100**, 1244—1251 (2006).
- Wang B. D., Yang Z. Y., Li T. R., *Bioinorg. Med. Chem.*, **14**, 6012—6021 (2006).
- Wu J. Z., Yuan L., Wu J. F., *J. Inorg. Biochem.*, **99**, 2211—2216 (2005).
- Hong D., Jun L., Kang C. Z., Yi Y., Hui C., *Inorg. Chim. Acta*, **358**, 3430—3440 (2005).
- Wang B. D., Yang Z. Y., Wang Q., Cai T. K., Crewdson P., *Bioorg. Med. Chem.*, **14**, 1880—1888 (2006).
- Kumar C. V., Barton J. K., Turro M. J., *J. Am. Chem. Soc.*, **107**, 5518—5523 (1985).
- Efink M. R., Ghiron C. A., *Anal. Biochem.*, **114**, 199—206 (1981).
- David S. S., Abhijit M., David M. P., *Chem. Rev.*, **93**, 2295—2316 (1993).
- Satyanarayana S., Dabrowiak J. C., Chaires J. B., *Biochemistry*, **32**, 2573—2584 (1993).
- Winterbourn C. C., *Biochem. J.*, **182**, 625—628 (1979).
- Winterbourn C. C., *Biochem. J.*, **198**, 125—131 (1981).